Arabian Journal of Chemistry (2016) 9, S1943–S1950

King Saud University

Arabian Journal of Chemistry

www.ksu.edu.sa
www.sciencedirect.com

ORIGINAL ARTICLE

New Mn(II), Ni(II), Cd(II), Pb(II) complexes with 2-methylbenzimidazole and other ligands. Synthesis, spectroscopic characterization, crystal structure, magnetic susceptibility and biological activity studies

Shayma A. Shaker [a,*], **Hamid Khaledi** [b], **Shiau-Chuen Cheah** [c], **Hapipah Mohd Ali** [b]

[a] *Department of Petrochemical Engineering, Technical College of Engineering, Duhok Polytechnic University, Duhok, Kurdistan Region, Iraq*
[b] *Chemistry Department, Faculty of Science, University of Malaya, 50603 Kuala Lumpur, Malaysia*
[c] *Centre of Natural Products and Drugs Discovery Research (CENAR), Department of Pharmacology, Faculty of Medicine, University of Malaya, Malaysia*

Received 27 January 2012; accepted 12 June 2012
Available online 4 August 2012

KEYWORDS

2-Methylbenzimidazole complexes;
Benzotriazole complexes;
N-acetylglycine complexes;
Biological activity;
Mixed ligand complexes

Abstract Synthesis and characterization of Mn(II), Ni(II), Cd(II) and Pb(II) mixed ligand complexes of 2-methylbenzimidazole with other ligands have been reported. The structure of the ligands and their complexes was investigated using elemental analysis, IR, UV–Vis, (^{1}H, ^{13}C) NMR spectroscopy, molar conductivity and magnetic susceptibility measurements. In all the studies of complexes, the 2-methylbenzimidazole behaves as a neutral monodentate ligand which is coordinated with the metal ions through the N atom. While benzotriazole behaves as a neutral bidentate ligand which is coordinated with the Ni(II) ion through the two N atoms. Moreover, the *N*-acetylglycine behaves as a bidentate ligand which is coordinated with the Mn(II), Ni(II) and Pb(II) ions through the N atom and the terminal carboxyl oxygen atom. The magnetic and spectral data indicate the tetrahedral geometry for Mn(II) complex, irregular tetrahedral geometry for Pb (II) complex and octahedral geometry for Ni(II) complex. The X-ray single crystal diffraction method was used to confirm a centrosymmetric dinuclear Cd(II) complex as each two metal ions are linked by a pair of thiocyanate N = S bridge. Two 2-methylbenzimidazole N-atom donors

* Corresponding author. Tel.: +6 03 8921 7241.
E-mail address: drshaimaa611@yahoo.com (S.A. Shaker).
Peer review under responsibility of King Saud University

Production and hosting by Elsevier

http://dx.doi.org/10.1016/j.arabjc.2012.06.013

and one terminal thiocyanate N atom complete a highly distorted square pyramid geometry around the Cd atom. Besides, different cell types were used to determine the inhibitory effect of Mn(II), Ni (II), Cd(II) and Pb(II) complexes on cell growth using MTT assay. Cd(II) complex showed cytotoxic effect on various types of cancer cell lines with different EC_{50} values.

1. Introduction

Benzimidazole derivatives are used in a great variety of biological processes and they are very important classes which have pharmacological effects and pharmaceutical drugs such as, antimicrobial, antifungal, antiviral, antihistaminic, antitumoral and anthelmintic activities and inhibition of nucleic acid synthesis (Shayma et al., 2011a; Ricardo and Samuel, 2008; Fatma et al., 2003). Moreover, the reactivity and property of the metal complexes with benzimidazole derivatives have been studied over the last decades, a few cases that involved the interaction of benzimidazole and benzotriazole with some metal complexes are known (Ricardo and Samuel, 2008; Shayma et al., 2010a; Reginaldo et al., 2001). Thus, the imidazole derivatives are playing a remarkable role in the structures and functions of a number of biologically important molecules (Senay and Cevdet, 1999). They are used as ligands toward transition ions with different biological molecules like vitamin B_{12} and several metalloproteins (Ricardo and Samuel, 2008; Reginaldo et al., 2001). However, the chemical properties, structures and reactivities of a number of azole- based transition metal complexes have shown a great utility in synthetic organic chemistry and catalysis (Doo et al., 2008). In this paper, four Mn(II), Ni(II), Cd(II) and Pb(II) complexes with 2-methylbenzimidazole and other ligands like *N*-acetylglycine are prepared and characterized by IR, UV–Vis spectra, magnetic property, X-ray diffraction and studied. Moreover, the biological activity of the above complexes has been reported. Keeping this in view, both FTIR and molecular modeling could be applied to interrupt the possible interaction of metals with organic structures (Ibrahim, 2009; Ibrahim et al., 2010; Ibrahim and Hanan, 2005).

2. Experimental

2.1. Material and measurements

All chemicals used in this study were obtained from commercial sources and used without further purifications ($MnCl_2$ $4H_2O$, $NiCl_2$ $6H_2O$, $CdCl_2$ H_2O, $Pb(NO_3)_2$ obtained from BDH. (2-Methylbenzimidazole, benzotriazole, *N*-acetylglycine, ethanol, DMSO) obtained from Merck.

Measurement of UV–Vis spectra was carried out using a Shimadzu UV–Vis spectrophotometer UV-160 in 10^{-3} M DMSO solution. IR spectra (KBr disc) in the region of 4000–400 cm^{-1} were recorded using a Shimadzu FTIR 8400 S Fourier transform infrared spectrophotometer. ^1H NMR, ^{13}C NMR spectra were recorded using a Bruker DPx-400 spectrophotometer relative to the internal standard, tetramethylsilane (TMS). Philips pw 9526 digital conductivity meter was used to measure molar conductivity. The magnetic susceptibility was measured at 25 °C using a balance magnetic susceptibility apparatus MK1. Elemental analysis (C, H, N) was performed on a Perkin Elmer B-240 Elemental Analyzer. Determination of metals was carried out using an Atomatic absorption spectrometer A-Analysis 800 Perkin Elmer. Finally, the melting points were determined using a stuart-melting point apparatus. Crystal data collection: *APEX2* (Bruker, 2006); Cell refinement: *SAINT* (Bruker, 2006); data reduction: *SAINT*; program used to solve structure: *SHELXS* 97 (Sheldrick, 2008); program used to refine structure: *SHELXL*97 (Sheldrick, 2008); molecular graphics: xp in SHELXTL (Sheldrick, 2008); software used to prepare material for publication: *SHELXL97* and *publCIF* (Westrip, 2010).

2.2. Preparation of $[Cd_2(B)_4(NCS)_4]$

An ethanolic solution (15 ml) of 2-methylbenzimidazole (1.32 g, 10 mmol) was added to an aqueous solution (20 ml) of $CdCl_2$ H_2O (0.5 g, 2.5 m mol) followed by the addition of an aqueous solution (15 ml) of KSCN (0.49 g, 5 mmol). The mixture was heated in a water bath for 30 min with constant stirring. The resulting precipitate was filtered off and recrystallized from ethanol to give the white crystals of Cd(II) complex (Shayma et al., 2010b).

2.3. Preparation of $[Mn(B)_2(Gly)]Cl$ and $[Pb(B)_2(Gly)]NO_3$

An ethanolic KOH solution (10 ml) of *N*-acetylglycine (Gly) (0.176–0.295 g) (1.5–2.51 mmol) and an ethanolic solution (12 ml) of 2-methylbenzimidazole (0.399–0.667 g) (3–5 mmol) were added respectively to an aqueous solution of metal salts, after constant stirring on water bath. The product precipitates immediately, filtered off, washed then recrystallized with 12 ml of ethanol and dried in an oven at 65 °C.

2.4. Preparation of $[Ni(B)_2(BT)(Gly]Cl$

An ethanolic solution (12 ml) of 2-methylbenzimidazole (0.556 g, 4 mmol) and an ethanolic solution (14 ml) of benzotriazole (0.25 g, 2 mmol) were added respectively to an aqueous solution of $NiCl_2$ $6H_2O$. An ethanolic KOH solution (12 ml) (0.246 g, 2 mmol) was added to the mixture with constant stirring. The product was immediately precipitated which was then filtered off, washed and recrystallized with ethanol (12 ml) and dried in an oven at 65 °C.

2.5. Cell culture

All the cells used in this study were obtained from American Type Cell Collection (ATCC) and maintained in a 37 °C incubator with 5% CO_2 saturation. A375 human melanoma, MCF-7 human breast adenocarcinoma cells and WRL-68 normal hepatic cells were maintained in Dulbecco's modified

Eagle's medium (DMEM). Whereas A549 non-small cell lung cancer cells were maintained in RPMI medium. Both medium were supplemented with 10% fetus calf serum (FCS), 100 units/mL penicillin, and 0.1 mg/ml streptomycin.

2.6. Cellular viability

Different cell types from above were used to determine the inhibitory effect of compounds CdB, MnB, NiBT and PbT on cell growth using the MTT assay. The MTT assay was *modified as described* by (Mosmann, 1983; Cheah et al., 2011). Briefly, cells were seeded at a density of 1×10^5 cells/mL in a 96-well plate and incubated for 24 h at 37 °C, 5% CO_2. Next day, cells were treated with the compounds respectively and incubated for another 24 h. After 24 h, MTT solution at 2 mg/mL was added for 1 h. Absorbance at 570 nm was measured and recorded using Plate Chameleon V microplate reader (Hidex, Turku, Finland). Results were expressed as a percentage of control giving percentage cell viability after 24 h exposure to test agent. The potency of cell growth inhibition for each test agent was expressed as an EC_{50} value, defined as the concentration that caused a 50% loss of cell growth. Viability was defined as the ratio (expressed as a percentage) of absorbance of treated cells to untreated cells.

2.7. Statistical analyses

Each experiment was performed at least two times. Results are expressed as mean value ± standard deviation (SD). Log EC_{50} calculations were performed using the built-in algorithms for dose–response curves with variable slope using GraphPad Prism software (version 4.0; GraphPad Software Inc., San Diego, CA). A fixed maximum value of the dose–response curve was set to the maximum obtained value for each drug.

3. Results and discussion

The prepared complexes were founded to be solid, soluble in DMSO. Elemental analyses C, H, N were found to be in agreement with the proposed molecular formula. Moreover, with exception of the Cd(II) complex all the metal complex solutions give electrolytic properties as indicated by their high molar conductivity which are given in Table 1 (Burger, 1973; Shayma et al., 2009, 2010c; Shayma, 2010b).

3.1. Electronic spectral studies and magnetic measurements

The electronic spectra of 2-methylbenzimidazole (B) in DMSO show bands at 274, 280 nm and 350 nm which can be attributed to $\pi \rightarrow \pi^*$ and $n \rightarrow \pi^*$ respectively (Shayma, 2010a; Shayma et al., 2011). The benzotriazole (BT) spectrum shows two strong bands assigned to $\pi \rightarrow \pi^*$ and $n \rightarrow \pi^*$ at 273 nm and 312 nm respectively. The electronic spectra of *N*-acetylglycine (Gly) show band at 284 nm which is due to $\pi \rightarrow \pi^*$ and another band at 340 nm attributed to $n \rightarrow \pi^*$ (Shayma, 2010c).

The electronic spectra of Mn(II) complex displayed two bands in the visible region at 425 and 598 nm which attributed to the electronic transition $^6A_1 \rightarrow {}^4T_{2(G)}$ and $^6A_1 \rightarrow {}^4T_{1(G)}$ respectively. Thus the magnetic moment value is 4.652 B. M, demonstrates that the Mn(II) complex is paramagnetic and has high spin tetrahedral geometry (Lever, 1968).

The gray octahedral complex of Ni(II) shows three bands in the visible region at 450, 765 and 920 nm which are assigned due to $^3A_2g_{(F)} \rightarrow {}^3T_2g_{(F)}$ (ν1), $^3A_2g_{(F)} \rightarrow {}^3T_1g_{(F)}$ (ν2) and $^3A_2g_{(F)} \rightarrow {}^3T_1g_{(P)}$ (ν3) respectively. The ligand field parameter 10Dq is 10869 cm^{-1} for (ν1). Moreover, the interelectronic repulsion parameter B was calculated and found to be 179 cm^{-1}, this value is less than the free Ni^{2+} ion value of 1040 cm^{-1} which was due to overlapping and delocalization of electrons over the molecular orbital that encompasses both the metal and ligands, the nephelauxetic ratio $\beta = B/B^o = 0.172$ indicates appreciable covalent character in this ligand (Vidyavati et al., 2008; Antonio et al., 2008). The μ_{eff} value of Ni(II) d^8 was 2.451 B M, this value was in agreement with the expected value (Nicholls, 1984).

Finally, Cd(II) and Pb(II) complexes did not show any *d–d* electronic transition in the visible region but shows absorption bands at 279, 280 and 320, 345 and 350 nm which are attributed to the charge transfer MLCT. All the absorption bands were fully assigned in Table 2.

3.2. Infrared spectra studies

The important infrared frequencies exhibited by the ligands and their complexes are listed in Table 3. A comparison of IR spectra of the ligands with their complexes is based on earlier studies of similar ligand (Vidyavati et al., 2008). The spectrum of the free ligand B shows a broad strong band at 3160 cm^{-1} which is due to ν(NH) (Overberger et al., 1965; Rabiger and Joullie, 1964). Other bands were observed at 3040 cm^{-1} and 2830 cm^{-1} which can be attributed due to the ν(C–H) aromatic and aliphatic vibrations respectively (Cross and Alan, 1969; Dyer, 1965; Williams and Fleming, 1973). Moreover, the ν(C═N) band of the ligand B was observed at 1660 cm^{-1} and this band was shifted to the lower frequencies by 20–5 cm^{-1} in the spectra of the complexes. This indicates that the ligand B was coordinated with the metal ions through the N atom. However, the spectrum of BT exhibited a weak band at 3247 cm^{-1} which is due to ν(NH). Thus, the band appeared at 1500 cm^{-1} belongs to ν(N═N) in BT and was

Table 1 Shows colors, elemental analysis and molar conductivity of these complexes.

Complexes	Color	MP °C	Yield	Elemental analysis Calc. (Found)%				Molar conductance $Ohm^{-1}cm^2\ mol^{-1}$
				C	H	N	M	
$[Mn(B)_2(Gly)]Cl$	Brown	200–202	66	45.92 (44.8)	3.85 (3.01)	14.87 (14.22)	11.66 (10.98)	31.4
$[Ni(B)_2(BT)(Gly]Cl$	Gray	> 300	70	48.55 (48.37)	3.90 (2.75)	18.87 (17.44)	9.88 (9.14)	35
$[Cd_2(B)_4(NCS)_4]$	White	> 300	64	43.86 (43)	3.272 (2.60)	17.05 (16.96)	22.80 (22.09)	12.11
$[Pb(B)_2(Gly)]\ NO_3$	White	210–211	71	33.28 (32.84)	2.792 (2.34)	10.78 (10.75)	31.89 (30.77)	29.8

Table 2 The UV–Vis spectra and magnetic moment values of the free ligands and their complexes.

Compound	λ_{max} nm	Wave number (cm^{-1})	ε_{max} $L.mol^{-1}$ cm^{-1}	Assignment	μ_{eff} Calc. (found)
B	274	36496	2498	$\pi \rightarrow \pi^*$	–
	280	35714	2339	$\pi \rightarrow \pi^*$	
	350	28571	100	$n \rightarrow \pi^*$	
BT	273	36630	2447	$\pi \rightarrow \pi^*$	–
	312	32051	12	$n \rightarrow \pi^*$	
Gly	284	35211	415	$\pi \rightarrow \pi^*$	
	340	29411	1200	$n \rightarrow \pi^*$	
$[Mn(B)_2(Gly)]Cl$	278	35971	350	Charge transfer (C.T)	5.916 (4.652)
	425	23529	27	$^6A_1 \rightarrow {}^4T_{2(G)}$	
	598	16722	35	$^6A_1 \rightarrow {}^4T_{1(G)}$	
[Ni(B)2(BT)(Gly]Cl	280	35714	150	C. T	2.828 (2.451)
	450	22222	74	$^3A_2g_{(F)} \rightarrow {}^3T_1g_{(P)}$ (ν3)	
	765	13071	95	$^3A_2g_{(F)} \rightarrow {}^3T_1g_{(F)}$ (ν2)	
	920	10869	50	$^3A_2g_{(F)} \rightarrow {}^3T_2g_{(F)}$ (ν1)	
$[Cd_2(B)_4(NCS)_4]$	279	35842	850	$\pi \rightarrow \pi^*$	Diamagnetic
	320	31250	1013	$n \rightarrow \pi^*$	
	345	28985	640	C. T (M → L)	
$[Pb(B)_2(Gly)]$ NO_3	280	35714	750	$\pi \rightarrow \pi^*$	Diamagnetic
	350	28571	1156	C. T (M → L)	

Table 3 Fundemental infrared bands (4000–400 cm^{-1}) of the ligands and their complexes.

Compounds	ν (NH)	ν (NCS)	ν (N = C)	ν (N = N)	$\nu (COO)_{asy}$	$\nu (COO)_{sy}$	ν (M–N)	ν (M–O)
B	3160	–	1660	–	–	–	–	–
BT	3247	–	–	1500	–	–	–	–
Gly	3380	–	–	–	1740	1370	–	–
$[Mn(B)_2(Gly)]Cl$	3320	–	1655	–	1735	1360	550	490
$[Ni(B)_2(BT)(Gly]Cl$	3330	–	1640	1445	1735	1365	555	490
							500	470
$[Cd_2(B)_4(NCS)_4]$	3300	2075 2120	1645	–	–	–	–	475, 485, 500
$[Pb(B)_2(Gly)]$ NO_3	3325	–	1650	–	1730	1365	540	450

shifted to lower frequencies by 55 cm^{-1} in the spectra of Ni(II) complex (Shayma, 2010a; Cross and Alan, 1969; Dyer, 1965; Williams and Fleming, 1973). The infrared spectrum of (Gly) shows an absorption band at 3380 cm^{-1} which is due to ν (NH). On Mn(II), Ni(II) and Pb(II) complexes formation, this band was shifted to the lower frequencies by 60–50 cm^{-1}. So, it is noted both of the ν(COO) asymmetric and symmetric bands of the ligand Gly exhibited at 1740 and 1370 cm^{-1}. On Mn(II), Ni(II) and Pb(II) complexes these two bands were shifted to the lower frequencies by 10–5 cm^{-1}. This indicates that the ligand Gly was a bidentate ligand which coordinated with the metal ions through the N atom and a terminal carboxyl oxygen atom (Shayma, 2010c).

The potassium thiocyanate spectrum showed a very strong band at 2048 cm^{-1} which is a result of ν(C≡N). This band was shifted to 2060 and 2130 cm^{-1} in Cd(II) complex which attributed to the bridge group ν (Cd–NCS–Cd) and terminal group ν (Cd–NCS). Because the NCS group forms a bridge between two metal atoms, and the stretching frequency of a bridging group is generally higher than of a terminal group (Nakamoto, 1995; Socrates, 1980; Shayma and Yang, 2009). Moreover, all the complexes appeared as weak bands in the region 450–490 cm^{-1} which are due to ν (M–O) indicated that the ligand Gly was coordinated with the Mn(II), Ni(II) and Pb (II) complexes through the two O atoms. While, the bands between 500 and 550 cm^{-1} which are attributed to ν (M–N) indicate that the free ligands B, BT and isothiocyanate were coordinated with the metal ions through the N atom.

3.3. ^1H NMR spectral studies

The ^1H NMR spectra of the free ligand B show a signal proton at 12.3 ppm which is due to NH. This signal showed at 12 and 11.8 ppm in the Cd(II) and Pb(II) complexes respectively. Actually, the appearance of NH group in both the complexes confirmed that the coordination is impossible through N1. Thus the spectrum of the ligand B shows signal protons at 7.53, 7.17, 7.30 and 7.50 ppm which are attributed to H4, H5, H6 and H7 respectively. In the Cd(II) and Pb(II) complexes, the signals of H5 and H6 were shifted downward to 7.18–7.20 ppm and 7.32–7.39 ppm respectively. While the signals of H4 and H7 were shifted to higher values between 7.45–7.50 and 7.40–7.49 ppm respectively (Haggag, 2007; Belanger et al., 1997).

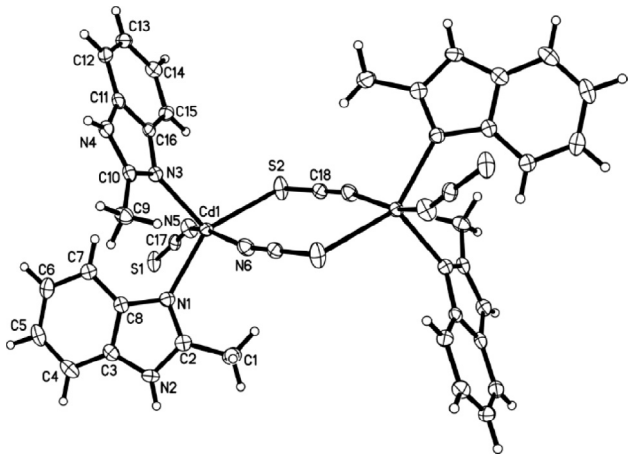

Figure 1 The molecular structure of $[Cd_2(B)_4(NCS)_4]$ showing displacement ellipsoids at the 50% probability level.

The *N*-acetylglycine shows single signal at 2.00 ppm which is due to the CH_3 group. Thus, the spectrum of the ligand shows two singlet signals at 6.34 and 4.01 ppm which could be due to NH and CH_2 groups respectively. In the Pb(II) complex the signal due to NH group was shifted downfield at 6.50 ppm. While, the signal of CH_2 group was shifted upfield at 3.35 ppm (Irene et al., 2006).

3.4. ^{13}C NMR spectral studies

The ^{13}C NMR spectra of the ligand B had shown signals at 130.1, 120.74, 113.62 and 140.9 ppm due to (C8, 9), (C5, 6), (C4, 7) and C2 respectively. On the Cd(II) and Pb(II) complexes, only the signal due to C2 was deshielded to the downfield by 11.60–11.53 ppm.

The ^{13}C NMR spectra of the ligand Gly exhibited signals at 179.3, 175.98, 45.20 and 25.55 pm due to C1, C3, C2 and C4 respectively. The signals of C1 and C2 were shifted downfield at 180.05 and 46.3 ppm respectively on the Pb(II) complex. These signals indicated that the *N*-acetylglycine was coordinated with the Pb(II) ion through the N and O atoms (Ramadan et al., 1997; Noriko et al., 2006).

Table 5 Hydrogen bond and angles.

Hydrogen-bond geometry (Å, °)				
D–H–J	D–H	H···A	D···A	D–H···A
N_2–H_2N···$S1^{ii}$	0.86 (2)	2.44 (2)	3.273(2)	163 (2)
N_4–H_4N···Sl^{iii}	0.84 (2)	2.48 (2)	3.281 (2)	159 (2)

Symmetry codes: (ii).

3.5. Crystal structure of $[Cd_2(B)_4(NCS)_4]$

Structure of the complexes is presented in Fig. 1 and the crystal data and structure refinement are listed in Table 4. Hydrogen bonding interactions in the crystal structure are given in Table 5.

3.6. Cytotoxic activity

To evaluate the cytotoxic activity, different single compounds namely CdB, MnB, NiBT and PbT were tested with a series of different doses on A375, A549, MCF-7 and WRL-68, respectively Fig. 2. After 24 h, cell viability was determined by the MTT assay. Test agents induced cell cytotoxicity in a

Table 4 Crystal data and structure refinement of $[Cd_2(B)_4(NCS)_4]$ complex.

Crystal data	
$[Cd_2(NCS)_4(C_8H_8N_2)_4]$	F(000) = 196S
M_T = 985.78	D_x = 1.641 Mg m^{-3}
Monoclinic, C2/c	Mo *Ka* radiation, λ = 0.71073 Å
Hall symbol: –C 2yc	Cell parameters from 4666 reflections
a = 18.1519(11) Å	θ = 2.3–30.1°
b = 10.2098(6) Å	μ = 1.32 mm^{-1}
c = 21.7385 (13) Å	*T* = 100 K
β = 97.864(1)°	Block, colorless
V = 3990.8 (4) Å^3	0.38 × 0.20 × 0.13 mm
Z = 4	
Data collection	
Broker APEXII CCD diffractometer	3593 independent reflections
Radiation source: fine-focus sealed tube	3213 reflections with $I > 2\sigma(I)$
Graphite	R_{int} = 0.022
φ and ω scans	θ_{max} = 25.2°, θ_{min} = 2.3°
Absorption correction: multi-scan *(SADABS:* Sheldrick, 1996)	*h* = -21 → 21
T_{min} = 0.634, T_{max} = 0.847	*k* = -12 → 8
9361 measured reflections	*l* = -26 → 26
Refinement	
Refinement on F^2	Primary atom site location: structure-invariant direct methods
Least-squares matrix: full	Secondary atom site location: difference Fourier map
$R[F^2 > 2\sigma(F^2)]$ = 0.021	Hydrogen site location: inferred from neighbouring sites
$wR(F^2)$ = 0.047	H atoms treated by a mixture of independent and constrained refinement
s = 1.03	$w = 1/[\sigma(F_o^2) + (0.0169P)^2 + 6.0676P]$ where $P = (F_o^2 + 2F_c^2)/3$
3593 Reflections	$(\Delta/\sigma)_{max}$ = 0.003

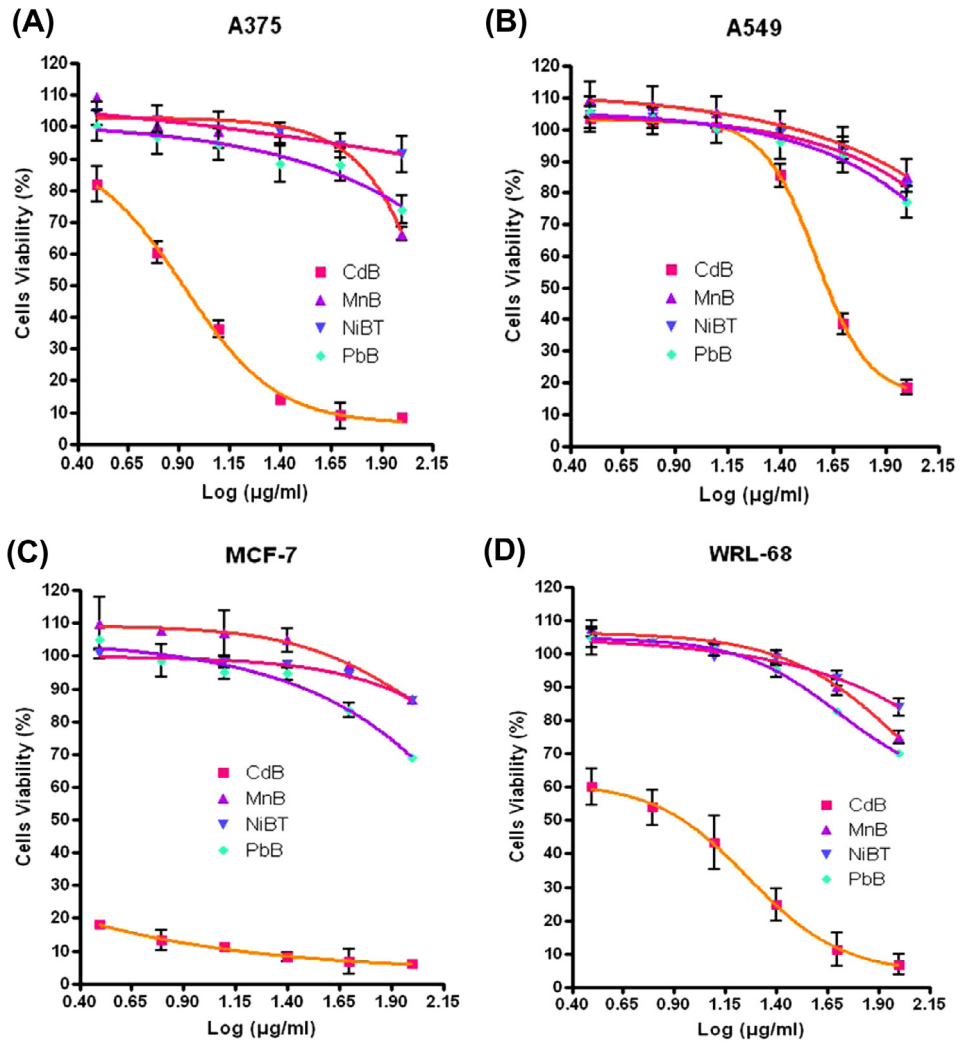

Figure 2 Dose–response curves (using GraphPad Prism) tested with Mn(II), Ni(II), Cd(II) and Pb(II) complexes in the MTT assays toward A) A375, B) A549, C) MCF-7, D) WRL-68 where MnB = $[Mn(B)_2(Gly)]Cl$, NiBT = $[Ni(B)_2(BT)(Gly]Cl$, CdB = $[Cd_2(B)_4(NCS)_4]$ and PbB = $[Pb(B)_2(Gly)]\ NO_3$.

concentration dependent manner. These dose titration curves allowed determining EC_{50} for the test agents toward different cell lines Table 6.

From Fig. 2 CdB showed cytotoxic effect on several of the cancer cell lines with different EC_{50} values. Cd(II) complex induced cell cytotoxicity in a concentration dependent manner. These dose titration curves allowed determining EC_{50} for the various compounds toward different cell lines. Cd(II) complex demonstrated dose-depended cytotoxic effects with EC_{50} values of 8.404 ± 1.4, 45.36 ± 3.7, 5.7 ± 0.9, and 6.7 ± 0.7 µg/mL; in A375, A549, MCF-7 and WRL-68, respectively.

However, Mn(II), Ni(II) and Pb(II) complexes showed no cytotoxic effect on different cell lines. These results indicate that cell lines differ in their sensitivity to the same test agent, which may be determined by multiple cell type-specific signaling cascades and transcription factor activities.

Cytotoxic screening models provide important preliminary data to select plant extracts or natural compounds with potential anticancer properties. In this study, the cytotoxic effect of Cd(II) complex was investigated by the addition of the MTT tetrazolium salt to various cancer cell lines previously treated with Cd(II) complex. Taken together, the cytotoxic effects exerted by Kunstlerone as a promising compound suggest its potential as anti-proliferation agent. To our knowledge, the cytotoxic potentials of Cd(II) complex have not been examined and the underlying molecular mechanisms remain to be discovered (Mosmann, 1983; Cheah et al., 2011).

Table 6 Effect of CdB, MnB, NiBT and PbT on different cells type expressed as EC_{50} values in 24 h MTT assay.

Cell line	EC50 ± S.D (µg/mL)			
	A375	A549	MCF-7	WRL-68
$[Mn(B)_2(Gly)]Cl$	> 100	> 100	> 100	> 100
$[Ni(B)_2(BT)(Gly]Cl$	> 100	> 100	> 100	> 100
$[Cd_2(B)_4(NCS)_4]$	8.404	45.36	5.7	6.7
$[Pb(B)_2(Gly)]\ NO_3$	> 100	> 100	> 100	> 100

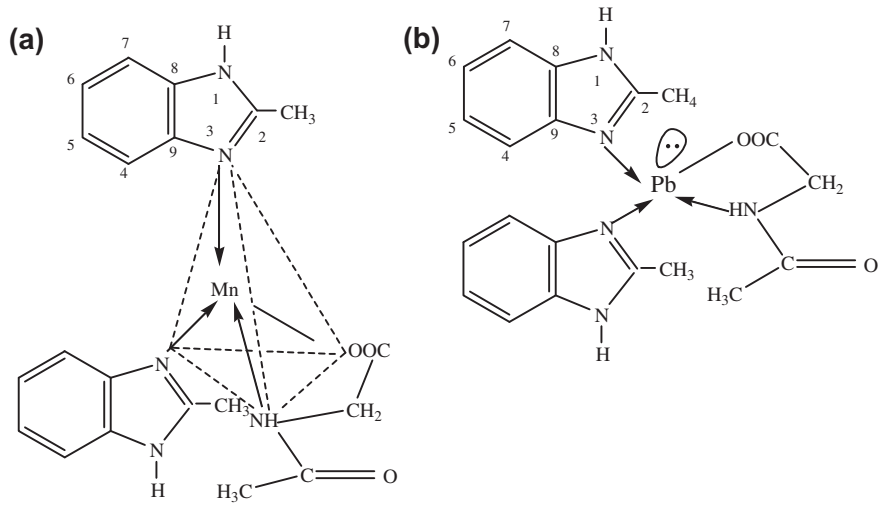

Figure 3 (a) Structure of the $[Mn(B)_2(Gly)]Cl$ complex and (b) Structure of $[Pb(B)_2(Gly)]NO_3$.

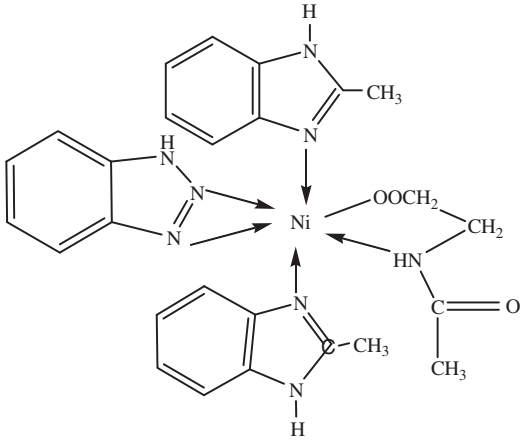

Figure 4 Structure of $[Ni(B)_2(BT)(Gly]Cl$.

4. Conclusion

In this paper, new mixed ligand complexes containing 2-methylbenzimidazole, benzotriazole, *N*-acetylglycine and isothiocyanate with Mn(II), Ni(II), Cd(II) and Pb(II) ions were synthesized. All the complexes with the exception of Cd(II) complex show electrolytic properties. Elemental analysis, magnetic susceptibility, FTIR, UV–Vis spectral observation suggested the tetrahedral geometry around Mn(II) complex as shown in Fig. 3a, irregular tetrahedral geometry around Pb (II) complex as shown in Fig. 3b and octahedral geometry around Ni(II) complex as shown in Fig. 4. The X-ray structure analysis confirmed the distorted square pyramid geometry around each Cd(II) ion. Moreover, the Mn(II), Ni(II) and Pb(II) complexes showed no cytotoxic effect on different cells. While Cd(II) complex showed cytotoxic effect on various types of cancer cell lines with different EC_{50} values.

Acknowledgement

The authors thank the University of Malaya for funding this research study (UMRG Grant No. RG024/09BIO and FRGS Grant No. FP004/2010B).

References

Antonio, S.P., Nuria, C., Jaime, R., Maria, L.D., José, A.G., Antonio, S., 2008. Polyhedron 27, 3391–3397.
Belanger, S., Fortin, S., Beauchamp, A.L., 1997. Canadian Journal of Chemistry 75, 37–45. http://dx.doi.org/10.1139/v97-005.
Bruker, 2006. APEX2 (version 1.2 a) and SAINT (version 7.23 A). Bruker AXS Inc., Madison, WI, USA.
Burger, K., 1973. Coordination Chemistry Experimental Methods. Bult worths and Co publisher Ltd., London, 1973.
Cheah, S.C., Appleton, D.R., Lee, S.T., Lam, M.L., Hadi, A.H., Mustafa, M.R., 2011. Molecules 16, 2583–2598.
Cross, A.D., Alan, J., 1969. An Introduction to Practical Infrared Spectroscopy, third ed. Springer, Berlin.
Doo, H.J., Won, J.P., Jong, H.J., David, G.C., Hyosun, L., 2008. Inorganic Chemistry Communications 11, 1170–1173.
Dyer, R.J., 1965. Applications of Absorption Spectroscopy of Organic Compounds. Englewood Cliffs, NJ Prentice-Hall, USA.
Fatma, G.O., Gökc, E., Hatice, E., Nuran, D., Sibel, G., Aykut, O., 2003. European Journal of Medicinal Chemistry 38, 473–480.
Haggag, S.S., 2007. Indian Journal of Chemistry section 46A, 582–588.
Ibrahim, M., 2009. Journal of Computational and Theoretical Nanoscience 6, 682–685.
Ibrahim, M., Al-Hossain, A., Al-Fifi, Z., 2010. Journal of Computational and Theoretical Nanoscience 10, 2240–2244.
Ibrahim, M., Hanan, E., 2005. International Journal of Environment and Pollution 23, 417–424.
Irene, A., Juan, F., Roberto, L., Antonio, M., Violeta, S., 2006. European Journal of Inorganic Chemistry, 948–957.
Lever, A.B.P., 1968. Inorganic Electronic Spectroscopy. Elsevier publishing, NY, USA, New York.
Mosmann, T., 1983. Journal of Immunological Methods 65, 55–63.
Nakamoto, K., 1995. Infrared Spectra of Inorganic and Coordination Compounds. Wiley, New York, NY, USA.
Nicholls, D., 1984. Complexes and First Row Transition Elements. American Elsevier, London.
Noriko, C.K., Rumi, Y., Akihiro, H., Akifumi, A., Kenj, N., 2006. Inorganica Chimica Acta 359, 4412–4416.
Overberger, C.G., Pierre, S.T., Vorchheimer, N., Lee, J., Yaroslavsky, S., 1965. Journal of the American Chemical Society 87, 296–301. http://dx.doi.org/10.1021/ja01080a028.
Rabiger, D.J., Joullie, M.M., 1964. Journal of Organic Chemistry 29, 476–482. http://dx.doi.org/10.1021/jo01025a502.

Ramadan, R.M., Hamza, M.S., Attia, A.S., 1997. Polyhedron 16, 229–233.
Reginaldo, C.R., Francisca, N.R., Henrique, E.T., 2001. The Journal of the Brazilian Chemical Society 12, 234.
Ricardo, I.C., Samuel, P.H.R., 2008. Journal of Molecular Structure 892, 477–484.
Senay, Y., Cevdet, Y., 1999. Vibrational Spectroscopy 21, 127–132.
Shayma, A.S., 2010a. E-Journal of Chemistry 7, 1598–1604.
Shayma, A.S., Hamid, K., Hapipah, M.A., 2010a. Acta Cryst E 66, o2913.
Shayma, A.S., Hamid, K., Hapipah, M.A., 2010b. Acta Cryst E 66, m1464.
Shayma, A.S., Yang, F., Abbas, A.S., 2009. European Journal of Scientific Research 33, 702–709.
Shayma, A.S., Yang, F., Sadia, M., Mohean, E., 2010c. Sains Malaysiana 39, 957–962.
Shayma, A.S., 2010b. E-Journal of Chemistry 7, S594–S600.
Shayma, A.S., Hamid, K., Hapipah, M.A., 2011. Chemical Papers 65, 299–307.
Shayma, A.S., 2010c. E-Journal of Chemistry 7, S580–S586.
Shayma, A.S., Yang, F., 2009. American Journal of Scientific Research 5, 20–26.
Sheldrick, G.M., 2008. Acta Crystallogr A 64, 112. http://dx.doi.org/10.1107/S0108767307043930.
Socrates, G., 1980. Infrared Characteristic Group Frequencies. Wiley, New York.
Vidyavati, R., Nirdosh, P., Angadi, S.D., 2008. E-Journal of Chemistry 5, 577–583.
Westrip, S.P., 2010. Journal of Applied Crystallography 43, 920–925.
Williams, D.H., Fleming, 1973. Spectroscopic Methods in Organic Chemistry, 2nd ed. McGraw-Hill, London, UK.